FULL PAPER DOI: 10.1002/adsc.201900709

Toward Automated Enzymatic Glycan Synthesis in a Compartmented Flow Microreactor System

Raphael Heinzler,[+a] Thomas Fischöder,[+b] Lothar Elling,[b,*] and Matthias Franzreb[a,*]

[a] Institute of Functional Interfaces, Karlsruhe Institute of Technology, Karlsruhe, Germany
Fax: (+ +49)-721-608-2-3478, phone: (+ +49)-721-608-2-3595
E-mail: Matthias.franzreb@kit.edu

[b] Laboratory for Biomaterials, Institute for Biotechnology and Helmholtz Institute for Biomedical Engineering, RWTH Aachen University, Aachen, Germany
Fax: (+ +49)-241-802-2387, phone: (+ +49)-241-802-8350;
E-mail: l.elling@biotec.rwth-aachen.de

[+] These authors contributed equally to this work

Manuscript received: June 7, 2019; Revised manuscript received: July 17, 2019;
Version of record online: ■■, ■■

Supporting information for this article is available on the WWW under https://doi.org/10.1002/adsc.201900709

Abstract: Immobilized microfluidic enzyme reactors (IMER) are of particular interest for automation of enzyme cascade reactions. Within an IMER, substrates are converted by paralleled immobilized enzyme modules and intermediate products are transported for further conversion by subsequent enzyme modules. By optimizing substrate conversion in the spatially separated enzyme modules purification of intermediate products is not necessary, thus shortening process time and increasing space-time yields. The IMER enables the development of efficient enzyme cascades by combining compatible enzymatic reactions in different arrangements under optimal conditions and the possibility of a cost-benefit analysis prior to scale-up. These features are of special interest for automation of enzymatic glycan synthesis. We here demonstrate a compartmented flow microreactor system using six magnetic enzyme beads (MEBs) for the synthesis of the non-sulfated human natural killer cell-1 (HNK-1) glycan epitope. MEBs are assembled to build compartmented enzyme modules, consisting of enzyme cascades for the synthesis of uridine 5′- diphospho-α- D-galactose (UDP-Gal) and uridine 5′-diphospho-α-D-glucuronic acid (UDP-GlcA), the donor substrates for the Leloir glycosyltransferases β4-galactosyltransferase and β3-glucuronosyltransferase, respectively. Glycan synthesis was realized in an automated microreactor system by a cascade of individual enzyme module compartments each performing under optimal conditions. The products were analyzed inline by an MS-system connected to the microreactor. The high synthesis yield of 96% for the non-sulfated HNK-1 glycan epitope indicates the excellent performance of the automated enzyme module cascade. Furthermore, combinations of other MEBs for nucleotide sugars synthesis with MEBs of glycosyltransferases have the potential for a fully automated and programmed glycan synthesis in a compartmented flow microreactor system.

Keywords: Glycoconjugate; Microreactors; Biocatalysis; Immobilization; Magnetic beads

Introduction

Carbohydrate molecules linked to other compounds such as proteins and lipids are called glycoconjugates and serve various functions, including cell-to-cell and cell-to-matrix communication as well as cross-linking between proteins.[1] For chemical stereoselective and regioselective glycosylations, multi-step syntheses are

necessary because the numerous hydroxyl groups present on individual sugars must be selectively protected and deprotected.[2] This is even more severe in case of an automated chemical glycan synthesis, as each step must be optimized for high product yields. Moreover, lengthy and time-consuming procedures are also required for the removal of by-products, such as stereoisomers, regioisomers, unreacted intermediates. Elegant strategies have been developed to address these challenges for automated chemical glycan synthesis leading up to hexasaccharides and even a 50mer of a homopolysaccharide.[3] However, yields are still low or moderate. In contrast, enzyme-assisted glycan synthesis is an attractive alternative to chemical synthesis as it has the advantage of achieving regio- and stereoselective glycosylations in a single step. Although strict enzyme substrate specificity appears as a disadvantage, a whole enzyme toolbox for glycosylation reactions and synthesis of nucleotide sugars as precursors of glycosyltransferases is now available for enzymatic synthesis of complex glycans.[4] Automated enzymatic synthesis is, therefore, an emerging and still developing technology. With glycosyltransferases in solution, automated glycan using solid-phase, polymer-bound[5] or tagged substrates for capture and release of products[6] have been developed, each strategy with its own pros and cons as discussed in recent reviews.[7] A common disadvantage is that glycosyltransferase reactions are not optimized for high product yields in short reaction time, and the precious biocatalysts are not recovered and reused. Relevant numbers for space-time-yield (STY, g product L^{-1} day^{-1}) and product-specific total turnover number TTN (g product/g catalyst) are therefore low for automated enzymatic synthesis. Only a few immobilized Leloir-type glycosyltransferases have been applied in glycan synthesis.[8] Key to high enzyme activity is the oriented immobilization on surfaces or polymers mediated by terminal peptides or proteins. Leloir-type glycosyltransferases and enzymes for nucleotide sugar synthesis have been immobilized via their polyhistidine tags.[9] Immobilized His-tagged enzymes can show activities close to those in solution due to the highly specific orientation provided by the His_6 linkage.[10] Magnetic particles are well suited as carriers because of their easy separation by magnetic fields, thus resulting in an enzyme-free product without time-consuming and expensive purification steps.

In addition, magnetic carriers simplify the implementation of automated processes and protocols, thus allowing the automation of complex multistep enzymatic cascades. A sophisticated example is demonstrated in this work by handling enzymes immobilized on magnetic particles in an automated compartmented flow microreactor system (CFMS). The principle of the CFMS was described before[11] illustrating the system well suitable for automated optimization of bioprocesses applying single immobilized enzymes, in this case, immobilized β1,4-galactosyltransferase. The reaction progress can be monitored online with spectroscopic methods and the temperature can be controlled precisely.

The herein used enzyme modules (EM) have been optimized and combined in our previous studies employing soluble enzymes (Scheme 1A). Galactokinase (GalK) was combined with UDP-sugar pyrophosphorylase (USP) in an enzyme cascade reaction for the synthesis of UDP-galactose (UDP-Gal, **3**) from D-(+)-galactose (Gal,**1**) via α-D-galactose-1-phosphate (Gal-1-P, **2**) in the EM-UDP-Gal.[12] In the EM-UDP-GlcA, UDP-glucose-dehydrogenase (UGDH) generates Uridine 5′-diphosphate-glucuronic acid (UDP-GlcA, **5**) from UDP-glucose (UDP-Glc, **4**), while NADH oxidase (NOX) regenerates the co-substrate NAD^+.[13] In the EM-GalT, β1,4-galactosyltransferase (GalT) transfers galactose from UDP-Gal onto a *tert*-butyloxycarbonyl protected *N*-acetylglucosamine (GlcNAc-linker-*t*Boc, **6**) to synthesize *N*-Acetyl-D-lactosamine (LacNAc-linker-*t*Boc, **7**).[14] The UDP-GlcA, produced in the EM-UDP-GlcA, was used for glucuronosyltransferase (GlcAT) to transfer the GlcA onto LacNAc-linker-*t*Boc in the EM-GlcAT, resulting in the product non-sulfated human natural killer cell-1 (HNK-1) epitope (**8**).[15]

In this work, we demonstrate automated enzymatic glycan synthesis by enzyme cascade reactions, conducted in the CFMS, using six different enzymes immobilized on magnetic particles (Scheme 1A). Nucleotide sugars are synthesized in parallel enzyme modules (EM) and subsequently delivered to the reaction of two glycosyltransferases to synthesize the final product **8** with a yield of 96% (Scheme 1B). Product formation of individual glycosyltransferase steps was confirmed by an inline MS-system. To the best of our knowledge, such a high number of magnetic enzyme beads (MEB) has not yet been employed for biocatalytic cascades before; it is the first example for automated glycan synthesis in a compartmented microfluidic microreactor.

Results and Discussion

Enzyme Loading Yields of the Immobilization Step

Table 1 displays an overview of the loading yields of the PureCube Ni–IDA particles for all tested enzyme amounts, expressed as theoretical loadings in g immobilized enzyme per L settled beads. For UGDH the loading yields varied between 58% and 67% and for NOX between 56% and 80%. The loading yields of GalK, GalT, and GlcAT were around the same range of 73%–93%. Immobilizing USP led to loading yields of nearly 100%. Analyzing correlations between loading yield and theoretical loading, UGDH, USP, and GlcAT

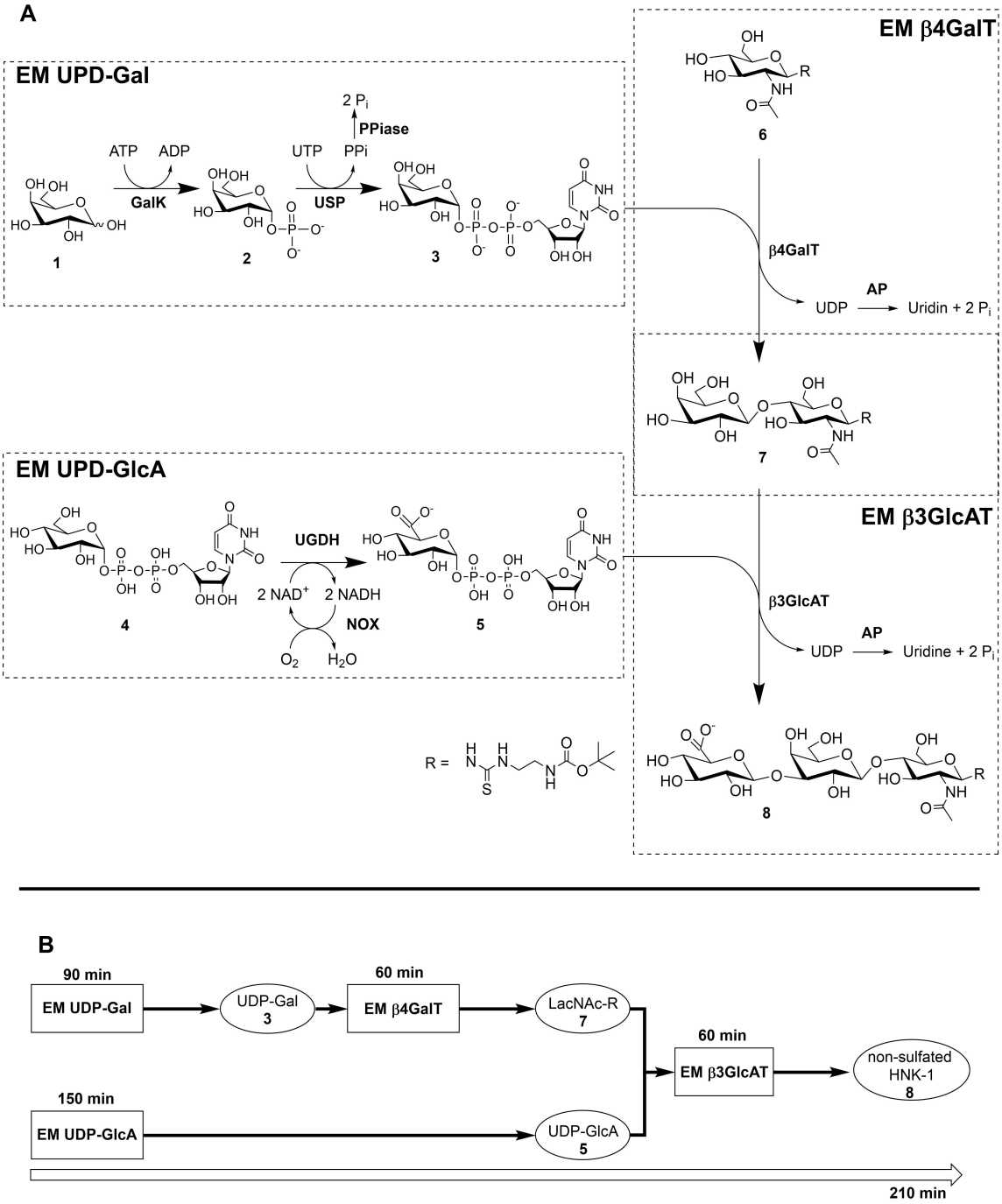

Scheme 1. Enzyme cascade using magnetic enzyme beads (MEB). **A**: Enzyme modules (dotted line) with magnetic enzyme beads (MEB) for the synthesis of the donor substrates UDP-Gal (**3**) and UDP-GlcA (**5**) were combined for glycosylation reactions by the glycosyltransferases β4GalT to yield LacNAc (**7**) and β3GlcAT for the synthesis of HNK-1 epitope (**8**). **B**: Flowchart of the reaction cascade in the compartmented flow microreactor system (CFMS). Box: reaction compartment with magnetic enzyme beads (MEB); circle: product compartment for transport to the next reaction compartment. Each compartment has a volume of 150 µL; EM reactions were carried out at 37 °C.

show a decreasing trend of the yield with increasing theoretical loading, the yield at 50 g/L being an exception. No correlation of loading yield and theoretical loading was found for immobilized NOX, GalK and GalT, if the 50 g/L tests are excluded. An increase of the loading yield with increasing theoretical loading would be unusual since the number of free binding sites decreases and more steric hindrance occur. For the reaction cascade in the CFMS, the 50 g/L MEB were used.

Table 1. Loading yields of all immobilized enzymes investigated. The first column shows the theoretical loading in g immobilized enzyme per L settled beads. The enzyme concentration used for immobilization was 0.15 g enzyme per L reaction solution in all cases.

Theoretical enzyme loading (g/L)	Loading yields of His_6-tagged enzymes [%] UGDH	NOX	GalK	USP	GalT	GlcAT
2.5	64	56	74	99	n.d.	n.d.
5	67	67	93	95	78	85
10	58	63	83	94	73	78
15	n.d[a]	n.d	n.d	n.d	76	73
30	56	70	n.d	n.d	n.d.	n.d.
50	64	80	87	94	84	86

[a] not determined.

Determination of the Optimum Reaction Parameters of the Magnetic Enzyme Beads MEB

To find the parameters giving the highest specific activity U/mg immobilized enzyme, for each immobilized enzyme, the effects of the reaction parameters were analyzed in a partially automated procedure in the CFMS in a 'one-factor-at-a-time' approach. The resulting optimal parameters of our immobilized enzymes and the optimal parameters of the respective free enzymes from literature are listed in Table 2. As can be seen, the values of the optimal reaction parameters for the immobilized enzymes largely correspond with those reported in the literature.[13,15–17]

The highest specific activity of immobilized UGDH, NOX, and GalK was achieved with the lowest loadings (see Figure S1, supporting information). By increasing the enzyme load, the specific activity decreased. This effect often occurs with immobilized enzymes and is explained by the fact that immobilized enzymes that are in close proximity to each other influence each other by steric hindrance. This impairs the binding of the substrates with the active sites and thus the activity.[19] In contrast, immobilized USP, GalT, and GlcAT displayed an increase of specific activity by rising enzyme loading. In this case, steric hindrance seems not to occur, which could be explained by a superior arrangement of these immobilized enzymes. The optimal values for pH and temperature did not differ much from published data.

The occurrence of the maximum specific activity at higher temperatures indicates a stabilization of the MEB against heat denaturation. In comparison with the literature, the Km value differed from around 2.5 times smaller to nearly 15 times higher and the v_{max} value from about 8 times smaller to more than two times higher (see Figure S2–S4, supporting information).

Table 2. Experimentally determined optimal reaction conditions and kinetic data, compared to data from the literature in brackets.

	UGDH	NOX	GalK	USP	β4GalT	β3GlcAT
pH-optimum	9.5 (9.7)	6 (6–6.5)	7.5 (7.5)	7.5 (7.5)	7.5 (7.5)	6.5 (6.5)
Temperature-optimum	40 °C (30 °C)	25 °C (30–40 °C)	40 °C (40 °C)	45 °C (45 °C)	40 °C (30 °C)	50 °C (45 °C)
Loading (theoretical)	2.5 g/L	2.5 g/L	5 g/L	50 g/L	50 g/L	15 g/L
v_{max}	UDP-Glc: 0.12 U/mg (0.81 U/mg)	$NADH + H^+$: 16.8 U/mg (116 U/mg)	Gal: 1.9 U/mg (5 U/mg)	Gal-1-P: 10.6 U/mg (13.1 U/mg)	GlcNAc-linker-*t*Boc: 0.68 U/mg (1.13 U/mg)	LacNAc-linker-*t*Boc: 1.1 U/mg (0.48 U/mg)
	NAD^+: 0.11 U/mg (0.92 U/mg)		ATP: 1.13 U/mg (6.5 U/mg)	UTP: 11.7 U/mg	UDP-Gal: 1.1 U/mg	UDP-GlcA: 1.2 U/mg (0.45 U/mg)
K_m	UDP-Glc: 0.09 mM (0.03 mM)	$NADH + H^+$: 0.37 mM (0.024 mM)	Gal: 1.54 mM (0.24 mM)	Gal-1-P: 1.1 mM (0.83 mM)	GlcNAc-linker-*t*Boc: 0.72 mM (3.07 mM)	LacNAc-linker-*t*Boc: 0.99 mM (0.24 mM)
	NAD^+: 0.16 mM (0.44 mM)		ATP: 0.7 mM (0.31 mM)	UTP: 1.6 mM	UDP-Gal: 5.4 mM	UDP-GlcA: 0.59 mM (0.19 mM)
K_i	–	–	Gal: 1.8 mM (33.1 mM) ATP: 3.15 mM (5.8 mM)	UTP: 1.87 mM	GlcNAc-linker-*t*Boc: 3.24 mM (2.66 mM)	–
Reference	[13,15]	[16,18]	[13]	[12]	[14,17]	[15]

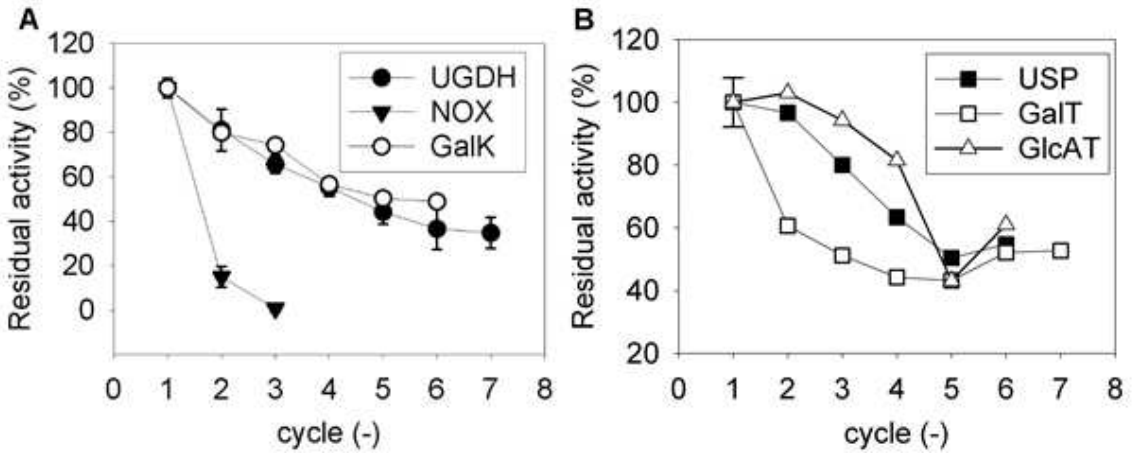

Figure 1. Reuse of immobilized (A) UGDH, NOX, GalK and (B) USP, GalT, GlcAT in multiple cycles.

The GalK, USP and GalT MEB displayed a substrate inhibition as stated in the literature for the free enzymes.[12,13,17] Immobilization via complex binding can cause a change in K_m values, for example, if the binding of the active site is impaired by the Ni–IDA functionalization of the magnetic particles. Also, if the immobilization causes the orientation of the catalytic center which is not optimal for the substrate to bind, the K_m value can change. In summary, the usefulness of the CFMS for semi-automated parameter screening and optimization of enzymatic reactions could be demonstrated with a multitude of different immobilized enzymes and tested parameters.

Recycling of the MEB

The results of the recycling of immobilized UGDH are shown as the percentage residual activity in Figure 1A). After the second cycle, 81% residual activity could be measured. Subsequently, it gradually decreased by 9% to 16%. During the fourth cycle, the residual activity of 55% was measured and in the seventh cycle about 35%. Wahl et al. achieved a residual activity of 50% after 3 h reaction time with free UGDH.[13] This corresponds to about six cycles, where the immobilized UGDH showed about 37% of the original specific activity. In the case of MEB loaded with NOX, the specific activity decreased by nearly 85% after the first recycling. Published data of free NOX already shows the low stability of NOX, with a half-life time of 10 min and 10–20% residual activity after 30 min.[13] The results of the repeated assays with immobilized GalK show a fairly constant decrease of the residual activity until the fifth cycle. At the last cycle, the residual activity of around 50% remains about the same. For the immobilized USP, the graph (see Figure 1B) shows a similar course, with a slightly higher residual activity of around 55% after six assays. The specific activity of immobilized β4GalT decreased by almost 40% after the first assay but reached an approximately constant residual activity of around 50% during the further cycles up to seven repetitions. Finally, the course of the residual activity of immobilized β3GlcAT did not change significantly for the first three cycles. Subsequently, the residual activity decreased to 61% at the sixth cycle with an outlier in the fifth cycle. In summary, with the exception of NOX, all other MEB showed a residual activity of around 40–60% after six or seven cycles. This offers the possibility for multiple reuses of the MEB also in complex enzymatic cascades, where the MEB could be easily recovered and replaced individually, while the use of free enzymes would lead to a mixture after the first run of the cascade with limited use for further runs.

Automated Enzymatic Glycan Synthesis

With optimal reaction conditions for MEB, the synthesis of the non-sulfated HNK-1 epitope in the reactor system was investigated. Different mixing ratios of MEB and substrate concentrations were investigated (see Figure S5A/B, supporting information). With 2 mM of the starting substrates **1** and **4**, EM-UDP-GlcA and EM-UDP-Gal reached conversions of 97.7% and 99.2%, respectively. The EM-GalT performed with 99.7% conversion of the available substrate **6**. Finally, after additional 60 min, the EM-GlcAT converted 98% substrate **7** from EM-GalT and 99.3% substrate **5** from EM-UDP-GlcA, resulting in a total yield of 96.3% for **8** with respect to initial substrate concentrations (Figure 2A). The respective HPLC analysis is displayed in Figure S6 in the supporting information.

Product formation in the MEB CFMS system (Scheme 1B) was analyzed by ESI-Q-ToF MS. The mass spectrum of the reaction solution before adding

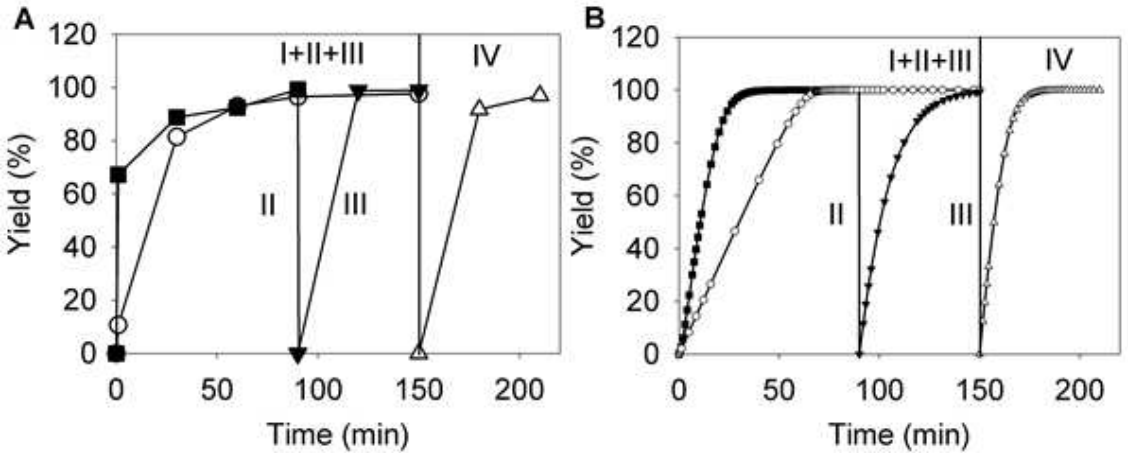

Figure 2. Yields of the optimized reaction cascade with MEB in the reactor system as (A) experimental, (B) simulated data. Applied enzyme modules: (I) EM-UDP-GlcA, (II) EM- UDP-Gal, (III) EM-GalT and (VI) EM-GlcAT. Intermediates and products: (-○-) UDP-GlcA (**5**), (-■-) UDP-Gal (**3**), (-▼-) LacNAc-linker-*t*Boc (**7**) and (-△-) non-sulfated HNK-1 epitope (**8**). For the substrates, 2 mM of UDP-Glc, Gal, ATP, UTP, GlcNAc-linker-*t*Boc, 4 mM NAD^+, 8 mM $MgCl_2$ and 6 mM $MnCl_2$ were used (see Table 3). The initial concentrations of the immobilized enzymes were 1 μg/μL for UGDH and NOX and 0.5 μg/μL for GalK, USP, GalT and GlcAT.

Table 3. Composition of the reaction mixtures utilized in the optimized reactor cascade experiments in the CFMS and in the approach with soluble enzymes. The volume of the EM-UDP-GlcA, EM-UDP-Gal and the reaction solution for the soluble enzymes was 150 μL respectively. All experiments were conducted at 37 °C.

Experiments (all numbers in mM)		Tris pH 8.7	Tris/KCl pH 7.5	UDP-Glc	NAD^+	Gal	ATP	UTP	$MgCl_2$	$MnCl_2$	GlcNAc-linker-*t*Boc
Reaction cascade in CFMS	EM-UDP-GlcA	100	–	2	4	–	–	–	–		–
	EM-UDP-Gal/ EM-GalT	–	100/ 25	–	–	2	2	2	8	6	2
Approach with enzymes in solution		–	100/ 25	2	4	2	2	2	8	6	2

β4GalT (Figure 3A) shows the substrate GlcNAc-linker-*t*Boc **6** with a molecular mass (*m/z*) of 422. The molecular mass *m/z* 444 Da derives from the sodium adduct replacing a proton by a sodium of the buffer solution. Transfer of galactose (180 Da) by β4GalT onto **6** results in a water molecule and the 162 Da bigger LacNAc-linker-*t*Boc **7** (Figure 3B). In the EM-GlcAT, the 194 Da GlcA from previously produced UDP-GlcA is transferred resulting in the 760 Da non-sulfated HNK-1 epitope **8** (Figure 3C).

For comparison, the same reaction sequence was performed with soluble enzymes with the same reaction solution composition (see Table 3). In contrast to the application of MEB, the soluble enzymes could not be separated from the reaction solution after use and remained in the solution during the following steps of the cascade. After 210 min, a total yield of 57.5% for **8** was achieved (Figure S5C, supporting information). The EM-UDP-Gal had the lowest yield of 75.5%, the EM UDP GlcA the highest of 100%. In the EM-UDP-Gal GalK had initially converted almost 91% of **1** and USP 83% of **2**, which led to the total yield of 75.5% for UDP-Gal **3**. The free β4GalT also converted almost 83% of **3**.

In comparison, the use of immobilized enzymes in the reactor system could synthesize almost 40% more non-sulfated HNK-1 epitope. The advantage of compartmentation is that optimal reaction conditions for a defined enzyme module are applied. In addition, the time- and cost-intensive removal of soluble enzymes from intermediate and final product volumes is not necessary with the MEB.

Theoretical Simulation of Automated Enzymatic Glycan Synthesis

In addition to the experimental work, the reaction cascade with MEB was also simulated based on the kinetic data obtained with single MEB systems (see Figure 2B). The simulated EM-UDP-GlcA and EM-UDP-Gal both achieved a conversion of 100%, whereby in the experiment the EM-UDP-GlcA had 97.7%

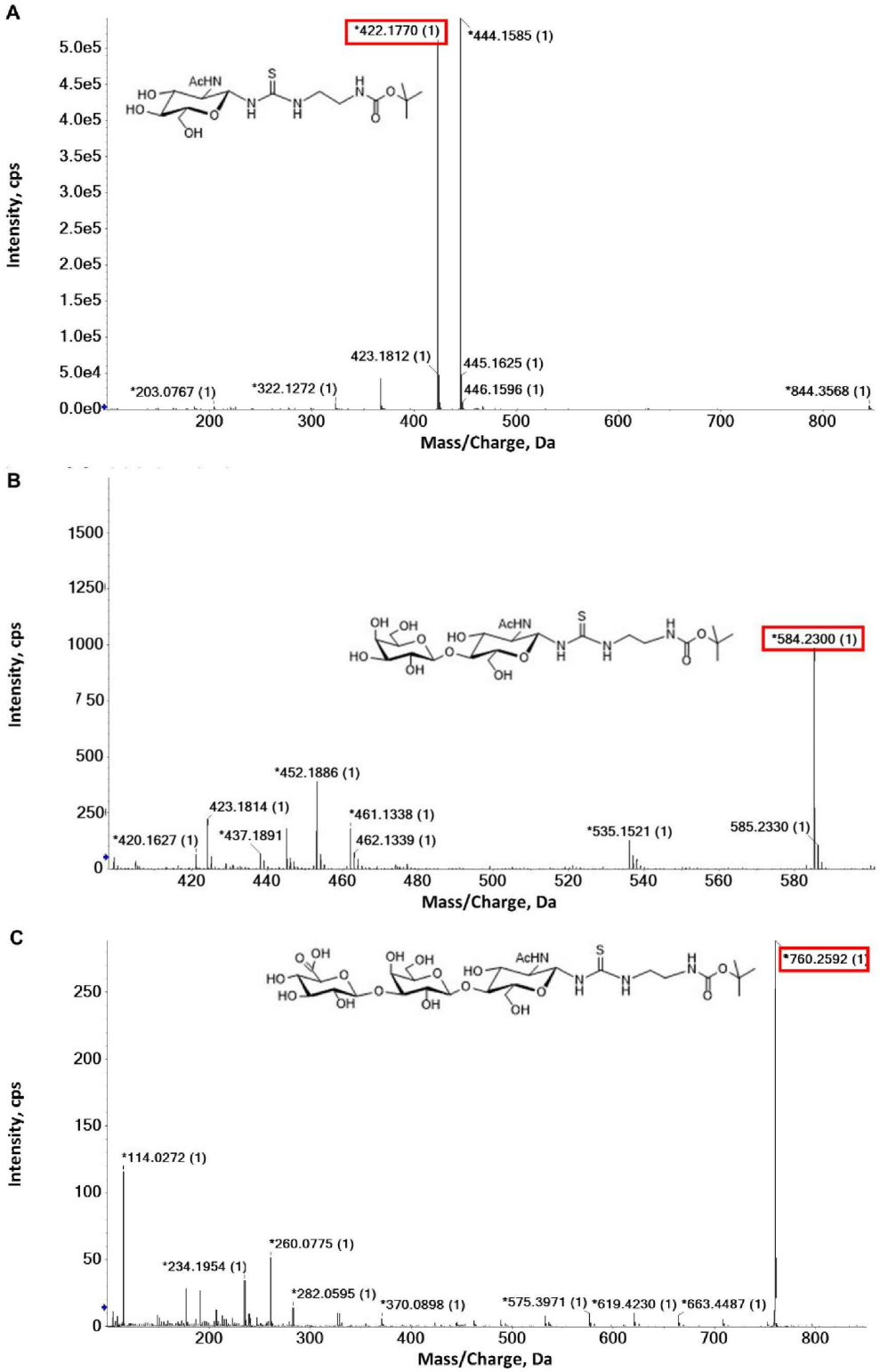

Figure 3. MALDI-TOF mass spectra of the substrates and products of each step of the cascade reaction of immobilized GalT and GlcAT. In A: the substrate GlcNAc-linker-*t*Boc (**6**) is marked, calculated mass (*m/z*): 422.2, in (B) the intermediate LacNAc-linker-*t*Boc (**7**): calculated mass (*m/z*): 584.2; (C) the product non-sulfated HNK-1 epitope (**8**): calculated mass (*m/z*): 760.3. All samples were diluted 1:10000.

and EM-UDP-Gal 99.2% conversion. Based on these substrate amounts, EM-GalT was simulated to convert 99.2%. In the experiment, EM-GalT surpassed the simulation and converted 99.7% of 6. Further, simulated EM-GlcAT converted 100% of the accessible substrate, which led to a total yield of 99.2%. The experimental EM-GlcAT converted 98% of 7 and 99.3% of 5, resulting in the total yield of 96.3% for 8.

The total turnover number (TTN) of the experiment is therefore 0.37 g product * g^{-1} of all immobilized enzymes and for the simulation 0.38 g product * g^{-1}. Thus, the simulation almost matches the experiment. Based on the experiment in the CMFS and the results of the recycling experiments, the reactor system would be able to produce in total 40 mg non-sulfated HNK-1 epitope in 18 h, which would be 6 cycles. It was assumed that a 3 mL compartment with 5 mM of substrates would be used and that six cycles with the same enzymes would be run. This would result in a space-time yield (STY) of HNK-1 epitope of 17.63 g * L^{-1} * day^{-1}. Considering the simulation, it can be possible to reach a STY of 18.16 g * L^{-1} * day^{-1}.

Conclusion

We here demonstrate for the first time glycan synthesis in an automated compartmented flow microreactor by a reaction cascade of six different magnetic enzyme beads. Compared to other published enzyme cascades in microreactors utilizing enzymes immobilized on magnetic beads,[20] the number of applied enzymes and the degree of automation is clearly increased, indicating the flexibility of the applied immobilization method and of the developed compartmented reactor device. Despite the high number of reaction steps, a yield of 96% non-sulfated HNK-1 epitope could be achieved. Thus, compared to an approach with soluble enzymes, the yield was almost 40% higher. This again demonstrates the great advantage of compartmentalization in the microreactor system, which can provide optimal reaction conditions for each reaction step and prevent inhibition. The microreactor system can product-specific to an MS-system for inline reaction control and product analysis. Due to the modularity and multiplexing of the microreactor system, the productivity could be increased by adding more tubes for parallel reactions or even more complex cascades consisting of more enzymes could be utilized. With further immobilized enzyme modules in hand, automated synthesis of more complex glycans can be realized in a compartmented flow microreactor.

Experimental Section

Magnetic Microcarriers

PureCube Ni–IDA MagBeads were purchased from Cube Biotech GmbH (Monheim am Rhein, Germany) and used as enzyme carriers without further modification. The ferrimagnetic magnetite beads are coated with 6% cross-linked agarose, functionalized with Ni–IDA and have a diameter of 25–30 µm. According to the manufacturer, the beads have a binding capacity of up to 70 mg (IDA) His-tagged protein/mL of settled beads.

Enzymes and Chemicals

The enzymes studied in this work are fusion constructs with an N-terminal polyhistidine (His_6)-tag. The enzyme production was done as described in our previous studies by Engels et al.[15] for UDP-glucose-dehydrogenase (UGDH, EC 1.1.1.22), NADH oxidase (NOX, EC 1.6.99.-) and β1,3glucuronyltransferase (β3GlcAT, EC 2.4.1.17, and by Wahl et al.[13] for galactokinase (GalK, EC 2.7.1.6) and for UDP-sugar pyrophosphorylase (USP, EC 2.7.7.64),[12] and by Fischöder et al.[14] for β1,4-galactosyltransferase (β4GalT, EC 2.4.1.38). The linker-modified substrate N-acetylglucosamine with a *tert*-butyloxycarbonyl protected amino group (GlcNAc-linker-*t*Boc) was kindly provided by Prof. Vladimír Křen (Institute of Microbiology, Czech Academy of Sciences).[21] The inhibitory by-products PP_i and UDP were removed by inorganic pyrophosphatase (PP_iase) and alkaline phosphatase (FastAP), respectively, purchased from Thermo Fisher Scientific (Rockford, USA). Standard compounds comprising Uridine 5′-diphosphate-α-D-glucose (UDP-Glc), nicotinamide adenine dinucleotide (NAD^+), nicotinamide adenine dinucleotide hydride (NADH), D-(+)-Galactose (Gal), adenosine 5′-triphosphate ATP, uridine 5′-triphosphate (UTP), α-D-Galactose-1-phosphate (G-1-P), Uridine 5′-diphosphate-α-D-galactose (UDP-Gal) and Uridine 5′-diphosphate-α-D-glucuronic acid (UDP-GlcA) were purchased from Sigma Aldrich (Deisenhofen, Germany) or VWR International GmbH (Bruchsal, Germany). All chemicals were analytical grade and used without further purification. The water used for all experiments was deionized and purified using a Milli-Q Ultrapure system from Merck Millipore KGaA (Darmstadt, Germany).

Immobilization of the Enzymes

Purified His_6-tagged enzymes were immobilized onto the IDA–Ni functionalized surfaces of the magnetic particles. For the immobilization, 5 µL particle slurry were used to bind 12.5/25/50/75/150/250 µg of the enzymes resulting in a theoretical loading of 2.5/5/10/15/30/50 g enzyme per L particle slurry. The immobilization reaction was performed at room temperature for 30 min in 1.5 mL Eppendorf tubes (Wesseling-Berzdorf, Germany) and done in duplicates, using 250 µL binding buffer. The binding buffer consisted of 20 mM Na_2PO_4/200 mM NaCl at pH 6.8. After the immobilization step, the samples were washed with (0.5 mL) 1 M NaCl buffer and twice with storage/binding buffer 1 (0.5 mL) 100 Tris/25 mM KCl buffer pH 7.5 or storage/reaction buffer 2 (0.5 mL) 50 mM Tris buffer pH 8.7 to desorb non-bound enzymes. The enzyme

particles were diluted to 10 µL particle slurry per mL storage buffer and stored at 4 °C. To calculate the amount of bound enzyme, the protein content in the incubation- and washing-supernatants was determined using the bicinchoninic acid (BCA) Protein Assay Reagent Kit from Thermo Scientific Pierce (Rockford, USA) according to manufacturer's instructions.

Activity Assay of Immobilized Enzymes in the CFMS

To characterize the activity of the MEB in the microreactor system with regard to pH, temperature, and loading, MEB were pumped into the reaction tubing of the system. The MEB were separated from the storage buffer (as described before),[22] resuspended in 100 µL of a preheated reaction buffer compartment and pumped to the temperature control module (TCM). Details of the IR-unit for preheating and the TCM are discussed by Heinzler et al.,[11] describing the reactor system. Compound composition for the activity assays of the analyzed enzymes are listed in Table S1 (supporting information). For each assay, 15 µg of MEB with a loading of 15 mg immobilized enzyme per mL settled beads were used in a 100 µL compartment. To avoid possible effects of enzyme deactivation, fresh MEB of the same batch were used in each assay, except for the assays on particle recycling. To test different temperatures, the activity of 15 mg/mL MEB was investigated at the respective optimal pH value of the free enzymes according to literature (UGDH/NOX/GalK,[13] USP,[12] GalT,[14] GlcAT[15]). The influence of different pH values was investigated at the respective optimal temperature of the free enzymes. Assays with various enzyme loadings were conducted at the optimal pH values and temperatures. For the kinetic studies, 15 mg/mL MEB were used at the optimal conditions with variable substrate concentrations. The kinetic constants were obtained by fitting a Michaelis-Menten equation $v = v_{max}*[S]/(K_m + [S])$ or a Michaelis-Menten equation including additional substrate inhibition $v = v_{max}/(1 + K_m/[S] + [S]/K_i)$ to the experimental data, using the software Sigma Plot 11 (Systat Software GmbH, Erkrath, Germany). If two substrates were used, the substrate, which was not varied in each case, was added in excess. Thus, limiting effects could be avoided and the corresponding kinetic parameters could be determined for each substrate. Assay conditions for kinetic studies are listed in Table S2 (supporting information). To determine the specific activity of the enzymes UGDH and NOX, the concentrations of the coproduct NADH in the samples were determined by measuring the absorption of the samples at 340 nm. For GalK, USP, GalT and GlcAT 30 µL of a sample of the sample were injected in an HPLC system (Agilent 1100 series, Waldbronn, Germany) and measured at 254 nm. For analytics of GalK and USP, a normal phase column (TSKgel Amide-80, Tosoh Bioscience, Germany, 5 µm, 2.0× 250 mm) was used and for analytics of GalT and GlcAT a reversed-phase column (SunFire, Waters, USA, 5 µm, 4.6× 150 mm). The concentration of the substrates/cosubstrates and the products/coproducts were calculated by the ratio of each peak area compared to the sum of the two peak areas and the corresponding calibration curve of standards. From the resultant concentrations, the activity was calculated by the increase of product over time. One enzyme unit correlates with one µmol product per minute. The mass-specific activity U/mg was calculated for one enzyme unit per mg immobilized enzyme.

Recycling of the MEB

To determine the recyclability of the different MEB, several activity assays were carried out in succession in which the MEB were reused. Between the reactions, the MEB were separated and washed three times with 200 µL reaction buffer. Thereafter, they were resuspended in a new reaction solution and transported to the TCM for the next cycle. To have enough volume for taking samples, a 300 µl compartment was used with the same compound and MEB concentration as stated before. The specific activity of the first assay of the respective enzyme was set as 100% residual activity.

Reaction Cascade in the CFMS

The reaction cascade (see Scheme 1B) was conducted in two separate tubes of the temperature control module (TCM) of the CFMS (Scheme S1A and B, supporting information) at 37 °C in 150 µL compartments. A compartment is an aqueous reaction solution, separated by ethyl acetate (EtOAc) and created by alternately pumping EtOAc and reaction solution within a tubing (see Scheme S1C, supporting information). The corresponding components of the reaction solutions of the compartments are listed in Table 3. The concentrations of the immobilized enzymes were 1 µg/µL for UGDH and NOX and 0.5 µg/µL for GalK, USP, GalT and GlcAT. Synthesis of UDP-GlcA was conducted for 150 min parallel to a synthesis of LacNAc-linker-*t*Boc. The reaction compartment EM-UDP-Gal contained MEB and 1 µL of 0.1 U/µL PP_iase to generate UDP-Gal within 90 minutes reaction time. After separation of MEB, the product compartment was transported to the MEB of the EM-GalT. The solution already contained the substrate GlcNAc-linker-*t*Boc and 1 U/µL FastAP was added to hydrolyze the byproduct UDP. GalT synthesized LacNAc-linker-*t*Boc within 60 minutes. In a similar way, UDP-GlcA was produced in a parallel reaction compartment within 150 min reaction time. After MEB separation, both product compartments were combined and added to the MEB of the EM-GlcAT. The synthesis was conducted for 60 minutes. The product concentrations were determined by HPLC.

For analytics of EM-UDP-GlcA, a reversed-phase column (TSKgel ODS-100V, Tosoh Bioscience, Germany, 4.6× 150 mm) was used. The mobile phase consisting of 30% (v/v) of 50 mM ammonium acetate (pH 4.5) in acetonitrile was used for 30 min at a flow rate of 0.3 mL*min^{-1}, increased after 10 min to 40% (v/v) in 5 min and after 5 min decreased in 2 min to 30% (v/v). At 260 nm, 30 µL of the sample were analyzed. The EM-UDP-Gal was analyzed with the normal phase column TSKgel Amide-80 using 20 mM tert-Butylamine as mobile phase at a flow rate of 0.9 mL*min^{-1}. In 35 min 10% (v/v) methanol was added. A sample of 30 µL was analyzed at 260 nm. Analytics of the EM-GalT and EM-GlcAT were done with the reversed-phase column SunFire with 24% (v/v) acetonitrile dissolved in MilliQ water with 0.1% formic acid as eluent at a flow rate of 0.3 mL*min^{-1}. For 30 min, 30 µL of sample mas measured at 254 nm.

In addition to the experiment in the CFMS, the reaction cascade was simulated with the application SimBiology (MathWorks, USA). The same reaction periods as in the experiment (see Scheme 1B) were used. The previously obtained kinetic data (see Table 2) were used as parameters for the simulation. For substrate concentrations, the same amounts were utilized as in the experiment (see Table 3).

For comparison, an experiment was conducted with the same amount of soluble enzymes in the same parallel reaction sequence using the same composition of the reaction solutions in the reactor system. The soluble enzymes were sequentially added to the reaction solutions for each EM. GalT was added to the reaction solution of EM-UDP-Gal after 90 min and subsequently incubated for a further 60 min. In parallel, the EM-UDP-GlcA was conducted for 150 min. The solutions of both reactions were combined and GlcAT was added. The reaction was stopped after 60 min, by adding 50 µL acetonitrile (ACN).

Inline Connection Between the Reactor and a Mass Spectrometer

To provide inline analytics, the reactor system was connected to an ESI-Q-ToF MS-System (QSTAR Pulsar I, SCIEX, USA) (see Scheme S2, supporting information). For this purpose, a syringe pump, an additional high-pressure multiport valve (Cetoni, Korbußen, Germany) and a mixing reservoir (1.5 mL Eppendorf tube, Wesseling-Berzdorf, Germany) were added to the reactor system. The syringe pump delivers samples to the mixing reservoir via the multiport valve, where they are diluted with Milli-Q water before being pumped into the MS system. Samples of the reaction solutions after 90 min, before starting the EM-GalT, after 150 min, before starting the EM-GlcAT, and at the end of the reaction cascade after 210 min were measured (Scheme 1B).

Acknowledgements

*The authors thank Prof. Dr. Vladimír Křen and co-workers (Academy of Science of the Czech Republic) for providing GlcNAc-linker-t*Boc. The authors gratefully acknowledge financial support by the Federal Ministry for Education and Research (BMBF) through the project "The Golgi Glycan Factory 2.0" (AZ: 031A557D and AZ: 031A557A) as part of the BMBF program Biotechnology 2020+-Basic Technologies and the support by Deutsche Forschungsgemeinschaft and Open Access Publishing Fund of Karlsruhe Institute of Technology.

References

[1] a) R. K. Yu, Y. Suzuki, M. Yanagisawa, *FEBS Lett.* **2010**, *584*, 1694–1699; b) K. Ohtsubo, J. D. Marth, *Cell* **2006**, *126*, 855–867.

[2] a) C.-C. Wang, J.-C. Lee, S.-Y. Luo, S. S. Kulkarni, Y.-W. Huang, C.-C. Lee, K.-L. Chang, S.-C. Hung, *Nature* **2007**, *446*, 896; b) X. Zhu, R. R. Schmidt, *Angew. Chem. Int. Ed.* **2009**, *48*, 1900–1934; *Angew. Chem.* **2009**, *121*, 1932–1967.

[3] a) C.-H. Hsu, S.-C. Hung, C.-Y. Wu, C.-H. Wong, *Angew. Chem. Int. Ed.* **2011**, *50*, 11872–11923; *Angew. Chem.* **2011**, *123*, 12076–12129; b) M. Guberman, P. H. Seeberger, *J. Am. Chem. Soc.* **2019**, *141*, 5581–5592; c) M. Panza, S. G. Pistorio, K. J. Stine, A. V. Demchenko, *Chem. Rev.* **2018**, *118*, 8105–8150.

[4] a) K. W. Moremen, A. Ramiah, M. Stuart, J. Steel, L. Meng, F. Forouhar, H. A. Moniz, G. Gahlay, Z. Gao, D. Chapla, S. Wang, J.-Y. Yang, P. K. Prabhakar, R. Johnson, M. d. Rosa, C. Geisler, A. V. Nairn, J. Seetharaman, S.-C. Wu, L. Tong, H. J. Gilbert, J. LaBaer, D. L. Jarvis, *Nat. Chem. Biol.* **2017**, *14*, 156; b) C. A. G. M. Weijers, M. C. R. Franssen, G. M. Visser, *Biotechnol. Adv.* **2008**, *26*, 436–456; c) I. Brockhausen, *Front. Immunol.* **2014**, *5*; d) P. Bojarová, V. Křen, *Trends Biotechnol.* **2009**, *27*, 199–209; e) L. Engels, L. Elling, Engels, in: *Handbook of Carbohydrate-Modifying Biocatalysts* (Eds.: P. Grunwald, ed.), Stanford Publishing, Stanford, **2016**, pp 297–320.

[5] a) P. Sears, C.-H. Wong, *Science* **2001**, *291*, 2344–2350; b) R. L. Halcomb, H. Huang, C.-H. Wong, *J. Am. Chem. Soc.* **1994**, *116*, 11315–11322; c) O. Blixt, T. Norberg, *J. Carbohydr. Chem.* **1997**, *16*, 143–154; d) T. Matsushita, I. Nagashima, M. Fumoto, T. Ohta, K. Yamada, H. Shimizu, H. Hinou, K. Naruchi, T. Ito, H. Kondo, S.-I. Nishimura, *J. Am. Chem. Soc.* **2010**, *132*, 16651–16656; e) X. Huang, K. L. Witte, D. E. Bergbreiter, C. H. Wong, *Adv. Synth. Catal.* **2001**, *343*, 675–681; f) J. Zhang, C. Chen, M. R. Gadi, C. Gibbons, Y. Guo, X. Cao, G. Edmunds, S. Wang, D. Liu, J. Yu, L. Wen, P. G. Wang, *Angew. Chem.* **2018**, *130*, 16880–16884.

[6] a) C. Cai, D. M. Dickinson, L. Li, S. Masuko, M. Suflita, V. Schultz, S. D. Nelson, U. Bhaskar, J. Liu, R. J. Linhardt, *Org. Lett.* **2014**, *16*, 2240–2243; b) J. Hwang, H. Yu, H. Malekan, G. Sugiarto, Y. Li, J. Qu, V. Nguyen, D. Wu, X. Chen, *Chem. Commun.* **2014**, *50*, 3159–3162; c) T. Li, L. Liu, N. Wei, J.-Y. Yang, D. G. Chapla, K. W. Moremen, G.-J. Boons, *Nat. Chem.* **2019**, *11*, 229–236.

[7] a) L. Wen, G. Edmunds, C. Gibbons, J. Zhang, M. R. Gadi, H. Zhu, J. Fang, X. Liu, Y. Kong, P. G. Wang, *Chem. Rev.* **2018**, *118*, 8151–8187; b) N. L. B. Pohl, *Nat. Chem.* **2019**, *11*, 201–203.

[8] a) T. Ito, R. Sadamoto, K. Naruchi, H. Togame, H. Takemoto, H. Kondo, S.-I. Nishimura, *Biochem.* **2010**, *49*, 2604–2614; b) K. Naruchi, S.-I. Nishimura, *Angew. Chem.* **2011**, *123*, 1364–1367; *Angew. Chem. Int. Ed.* **2011**, *50*, 1328–1331; c) N. Nagahori, K. Niikura, R. Sadamoto, M. Taniguchi, A. Yamagishi, K. Monde, S.-I. Nishimura, *Adv. Synth. Catal.* **2003**, *345*, 729–734.

[9] J. Nahalka, Z. Liu, X. Chen, P. G. Wang, *Chem. Eur. J.* **2003**, *9*, 372–377.

[10] T. Cha, A. Guo, X.-Y. Zhu, *Proteomics* **2005**, *5*, 416–419.

[11] R. Heinzler, J. Hübner, T. Fischöder, L. Elling, M. Franzreb, *Front. Bioeng. Biotechnol.* **2018**, *6*, 189.

[12] C. Wahl, M. Spiertz, L. Elling, *J. Biotechnol.* **2017**, *258*, 51–55.

[13] C. Wahl, D. Hirtz, L. Elling, *Biotechnol. J.* **2016**, *11*, 1298–1308.
[14] T. Fischöder, D. Laaf, C. Dey, L. Elling, *Molecules* **2017**, *22*, 1320.
[15] L. Engels, M. Henze, W. Hummel, L. Elling, *Adv. Synth. Catal.* **2015**, *357*, 1751–1762.
[16] W. Hummel, B. Riebel, *Biotechnol. Lett.* **2003**, *25*, 51–54.
[17] C. Rech, R. R. Rosencrantz, K. Křenek, H. Pelantová, P. Bojarová, C. E. Römer, F. G. Hanisch, V. Křen, L. Elling, *Adv. Synth. Catal.* **2011**, *353*, 2492–2500.
[18] Z. Findrik, A. Vrsalović Presecki, D. Vasić-Racki, *J. Biosci. Bioeng.* **2007**, *104*, 275–280; Presecki, D. Vasić-Racki, *J. Biosci. Bioeng.* **2007**, *104*, 275–280.
[19] Z. Guo, S. Bai, Y. Sun, *Enzyme Microb. Technol.* **2003**, *32*, 776–782.
[20] T. Peschke, M. Skoupi, T. Burgahn, S. Gallus, I. Ahmed, K. S. Rabe, C. M. Niemeyer, *ACS Catal.* **2017**, *7*, 7866–7872.
[21] B. Sauerzapfe, K. Křenek, J. Schmiedel, W. W. Wakarchuk, H. Pelantová, V. Křen, L. Elling, *Glycoconjugate J.* **2009**, *26*, 141–159.
[22] J. Hübner, R. Heinzler, C. Arlt, S. Hohmann, W. Brenner, M. Franzreb, *React. Chem. Eng.* **2017**, *2*, 349.

FULL PAPER

Toward Automated Enzymatic Glycan Synthesis in a Compartmented Flow Microreactor System

Adv. Synth. Catal. **2019**, *361*, 1 – 12

R. Heinzler, T. Fischöder, L. Elling*, M. Franzreb*